fibers

MDPI

Article

Properties of Composites from Curauá Fibers and High-Density Bio-Based Polyethylene: The Influence of Processing Methods

Daniele O. de Castro [1,†], Rachel P. O. Santos [1,2], Adhemar C. Ruvolo-Filho [3] and Elisabete Frollini [1,*]

[1] Macromolecular Materials and Lignocellulosic Fibers Group, Center for Research on Science and Technology of BioResources, São Carlos Chemistry Institute, University of São Paulo, P.O. Box 780, São Carlos 13560-970, SP, Brazil; danieleocastro@gmail.com (D.O.d.C.); rposantos@unaerp.br (R.P.O.S.)
[2] Materials and Environmental Process Optimization Research Group, Postgraduate Program in Environmental Technology, University of Ribeirão Preto, Ribeirão Preto 14090-000, SP, Brazil
[3] Department of Materials Engineering, Federal University of São Carlos, São Carlos 13565-905, SP, Brazil; adhemar@ufscar.br
* Correspondence: elisabete@iqsc.usp.br
† Current address: Tetra Pak, 221 86 Lund, Sweden.

Highlights

What are the main findings?

- The composites of bio-based high-density polyethylene (HDBPE), curaua fibers, and plant-based oils exhibited better properties when processed with a twin-screw extruder and injection molding rather than an internal mixer and thermopressing.
- The flexural properties and impact resistance demonstrated that castor oil, in comparison to canola oil and epoxidized soybean oil, performed better as a compatibilizer between hydrophilic fibers and a hydrophobic matrix.

What are the implications of the main findings?

- The optimal conditions identified for producing composites using HDBPE, curaua fibers, and plant-based oils are applicable to a range of other lignocellulosic fiber and thermoplastic polymer matrices.
- The methodologies and results outlined in this research can potentially drive the scalable fabrication of composites using bio-derived matrices, plant-based oils, and plant fibers.

Abstract: The study examined composites composed of curauá fibers (10%) and a high-density bio-based polyethylene (HDBPE) matrix, emphasizing the effects of processing methods on their final properties. In addition, plant-derived oils were applied as compatibilizers to improve the interfacial adhesion between the hydrophilic fibers and the hydrophobic HDBPE, thereby supporting the process's sustainability. The comparative analysis of HDBPE/curauá fiber/plant-based oil composites utilized distinct methodologies: compounding with an internal mixer, followed by thermopressing and mixture composition using a twin-screw extruder with subsequent injection molding. Castor oil (CO), canola oil (CA), or epoxidized soybean oil (OSE) were employed as compatibilizers (5%). All composites displayed high levels of crystallinity (up to 86%) compared to neat HDBPE (67%), likely due to interactions with curauá fibers and compatibilizers. The use of twin-screw extruder/injection molding produced composites with higher impact and flexural strength/modulus-assessed at 5%(approximately 222 J/m to 290 J/m; 22/700 MPa to 26/880 MPa, respectively), considerably exceeding those formed via internal mixer/thermopressing (approximately 110 J/m to 123 J/m; 14/600 MPa to 20/700 MPa). Micrographs of the composites indicated that the extruder separated the fiber bundles into smaller-diameter units, which may have facilitated the transfer of load from the matrix to

Academic Editors: Marija Gizdavic-Nikolaidis and Martin J. D. Clift

Received: 27 December 2024
Revised: 21 March 2025
Accepted: 31 March 2025
Published: 11 April 2025

Citation: de Castro, D.O.; Santos, R.P.O.; Ruvolo-Filho, A.C.; Frollini, E. Properties of Composites from Curauá Fibers and High-Density Bio-Based Polyethylene: The Influence of Processing Methods. *Fibers* **2025**, *13*, 45. https://doi.org/10.3390/fib13040045

the fibers, optimizing the composite's mechanical performance. As a compatibilizer, CO enhanced both properties and, when combined with the twin-screw extruder/injection technique, emerged as the optimal choice for HDBPE/curauá fiber composites.

Keywords: curauá fibers; bio-based polyethylene; vegetal-based oils; internal mixer/thermopressing molding; twin-screw extruder/injection molding

1. Introduction

Synthetic fibers, including glass fibers, carbon fibers, and metal fibers, are commonly employed by industries as reinforcing agents in polymer composites [1–4]. In contrast, polymer composites reinforced with plant fibers have also garnered extensive attention [5–8].

The utilization of lignocellulosic fibers in the manufacture of polymer composites is particularly appealing due to their low cost, the wide variety available in nature, and their suitability for high-volume applications [9–14].

The cellulose content of plant fibers plays a crucial role in determining their crystallinity and tensile properties, which subsequently affects their performance as reinforcements in polymer materials [8,15]. For this reason, curauá fibers were selected for the study, as they contain approximately 63% cellulose and have a crystallinity index of around 64% [16]. These characteristics make curauá fibers especially well suited for reinforcing polymer matrices when the objective is to incorporate plant fibers into composites.

Sourced from the curauá plant (*Ananas erectifolius*), which grows in the Amazon region, these fibers are valued in composite materials applications for their favorable processing characteristics, excellent specific mechanical performance, and low density [17–20]. Curauá was grown in agricultural fields near urban centers like Santarém in Pará, Brazil, in the Amazon region. The primary purpose of this cultivation was to produce fibers for the automobile industry [21]. The incorporation of curauá as a reinforcement in composites has the potential to broaden the scope of large-scale applications significantly. This development may enhance the market for these fibers and collaborate to foster economic growth within the region.

Curauá fiber-reinforced composites featuring a hydrophobic matrix, similar to many thermoplastics, exhibit certain limitations that need to be addressed before they can be widely adopted. The hydrophilic properties of curauá fibers pose challenges when combined with hydrophobic thermoplastic matrices, which may lead to insufficient interfacial adhesion [16,22].

The growing demand for alternatives to petroleum-based products has heightened the focus on bio-based polymers, especially in applications where renewability and biodegradability are crucial advantages. In this study, the composite matrices consist of bio-based high-density polyethylene (HDBPE), contributing to the capture and fixation of carbon dioxide (CO2) during production. Specifically, ethylene is derived from the dehydration of ethanol produced through the fermentation of sugarcane juice. Subsequently, polyethylene is synthesized from ethylene in a process involving fewer greenhouse gas emissions than the manufacturing process for fossil-based polyethylene, with approximately 2 kg of CO_2 being captured from the atmosphere for every kg of HDBPE produced [17,23]. Thus, HDBPE has a natural origin, is easily processed, and has the same physical properties as its equivalent petrochemical, in addition to having high ductility and water resistance, favoring its use in the production of composites [16,24]. It is essential to highlight that the global production capacity of bio-based plastics has more than doubled from 2010 to 2022, with approximately 2.2 Mt or 0.5% of the plastics in the worldwide market being

bio-based. It is also important to note that the share of bio-based polymers in total plastics production is increasing slightly yearly (from 0.54% in 2013 to 0.56% in 2022) as fossil-based plastics also increase [25]. These facts demonstrate the importance of valuing polymers of biological origin, such as HDBPE, in producing other materials, e.g., polymer composites reinforced by plant-based fibers [17].

Integrating plant fibers into a polymer matrix introduces a biodegradable component, thereby reducing the environmental impact typically associated with traditional polymers. Plant-based materials like lignocellulosic fibers serve as a nutrient source for microorganisms. These attracted microbes can decompose plant components, generating more opportunities for microbial colonization and enzymatic activity. The breakdown of fibers creates fissures, which facilitate the penetration of water, oxygen, and microbes deeper into the material. This interplay of factors, coupled with the degradation of the fibers themselves, can enhance the breakdown of the surrounding polymer [26]. The incorporation of plant fibers into polymer composites has the potential to reduce weight compared to using neat polymer, contingent upon the density of both the fibers and the polymer utilized. Plant fibers can also improve the material's acoustic and insulation properties [26]. These attributes render them potential candidates for applications within the field of civil construction.

The properties of the fiber–matrix interface in composite materials are critical in determining their overall characteristics, particularly their mechanical properties. This interface is vital in effectively transferring stress from the matrix to the reinforcing fibers. A robust interface facilitates efficient stress transfer, enhancing the composite's mechanical properties. Moreover, strong adhesion at this interface is essential to prevent phenomena such as fibers debonding, which can significantly undermine the structural integrity of the composite [27,28]. In this context, significant efforts have been undertaken to establish robust adhesion at the interface between hydrophilic plant fibers and a hydrophobic matrix. The treatment of fibers, whether chemical or physical, is an important research area focused on enhancing adhesion at the interface [29–33].

An alternative approach involves incorporating a small amount of compatibilizer to enhance the fracture resistance of thermoplastic composites. In this context, hydroxyl-terminated polybutadiene (LHPB) was used as a compatibilizer for HDBPE and curauá fibers [16]. Vegetal-based oils can also serve as compatibilizers due to their hydrocarbon chains, which have an affinity for hydrophobic polymers, and their polar groups, which can interact with the polar components of lignocellulosic fibers, namely, cellulose, hemicelluloses, and lignin (Figure 1). These compatibilizers are derived from renewable resources, aligning with efforts to produce materials through sustainable processes.

Santos et al. [34] studied the influence of the addition of 2.5 wt% castor oil (CO) on the composition of electrospun composite membranes of poly(ethylene terephthalate)/cellulose nanocrystals (CNCs). The authors observed that the composite membrane of nonaligned fibers containing 10 wt% CNCs and CO in its composition presented a tensile strength three-fold higher than pristine PET membrane, evidencing the effective performance of CO as a compatibilizing agent between the matrix/reinforcing agent [34].

Barbalho et al. [35] investigated HDBPE composites reinforced with NaOH-treated curauá fibers, utilizing polyethylene grafted with maleic anhydride (10 wt%) to intensify the interactions fiber–matrix at the interface. Their dynamic mechanical analysis (DMA) revealed that across the entire temperature spectrum from −40 °C to 100 °C, the composite incorporating HDBPE grafted with maleic anhydride and 5 wt% curauá fibers exhibited a storage modulus (E′) significantly superior to pure HDBPE. This investigation involved chemically modifying the polymer (using a reagent from a fossil source) and treating the fibers with an aqueous alkali solution, distinguishing it from the present study. To follow

investigating the performance of HDBPE composites reinforced with curauá fibers, in the present study, castor oil (CO, major component: ricinoleic acid triglyceride), canola oil (CA), or epoxidized soybean oil (OSE), Figure 1, was added to the matrix aiming to assess their role as compatibilizers [17]. Two distinct methodologies were employed to integrate these oils and fibers into molten HDBPE.

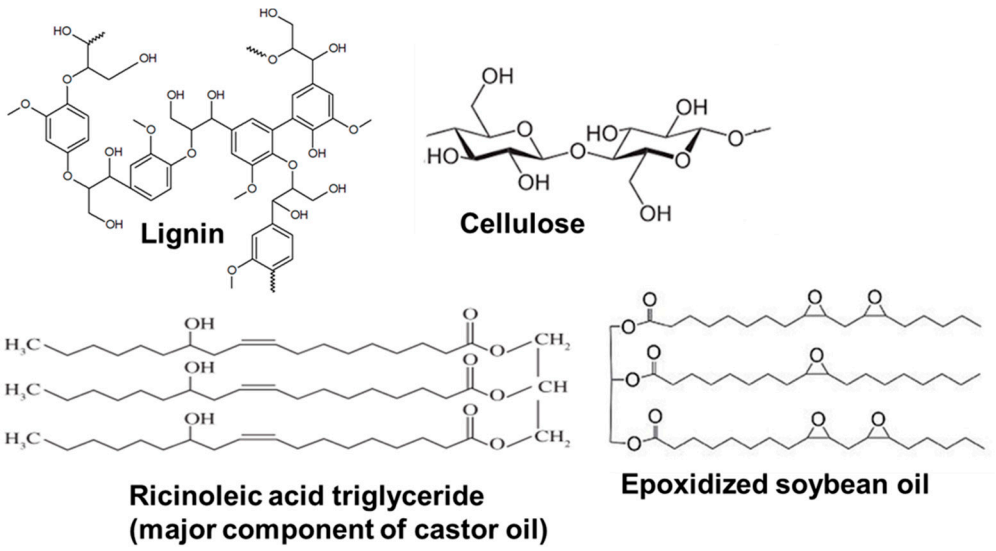

Figure 1. Chemical structures of lignin, cellulose, ricinoleic acid triglyceride, and epoxidized soybean oil.

Extrusion compounding is one of the most promising methods for industrial processing due to its easy scale-up and the possibility of further molding the materials [36,37]. Short fibers can be processed using extruders, followed by injection molding, and polymer composites can be continuously produced [38–42]. Extruders effectively disperse short fibers uniformly within the polymer matrix, resulting in consistent mechanical properties across the composite material. Additionally, their continuous operation and automation features can reduce production costs, enhancing efficiency in manufacturing processes [43]. Using an internal mixer can also effectively incorporate additives and/or fibers into molten polymers [44,45]. The resulting blend can then undergo thermopressing, a widely utilized method in the production of composite polymer parts [46]. Composites reinforced with natural fibers, such as those sourced from plants, can be manufactured utilizing either an internal mixer process or a twin-screw extrusion technique. Following these initial processing methods, subsequent operations like thermoforming or injection molding can be employed to finalize the production [47–49].

This study explored the characteristics of HDBPE composites reinforced with curauá fibers and utilized vegetal-based oils as compatibilizers to bridge the gap between the hydrophilic nature of the fibers and the hydrophobic polymer matrix. Two methodologies were employed to fabricate these composites, aiming to determine which method would more effectively enhance the impact of the vegetal-based oils as compatibilizers and improve the composites' properties, particularly impact resistance and flexural strength. The first approach involved compounding the materials in an internal mixer, followed by thermopressing to shape the composite [17]. The second method employed a twin-screw extrusion process, followed by shaping through injection molding.

As far as it is known, this study is the first of its kind.

2. Materials and Methods

2.1. Materials

HDBPE (SGF4950HS, "green polyethylene", melt flow rate of 0.10 ± 0.01 g/10 min, the density of 0.95 g/cm^3 [50]) from Braskem (Rio Grande do Sul, Brazil) was used in the present study. The plant-based oils (CO, CA, and OSE), and the curauá fibers sourced from plants cultivated in the Santarém region (density: 1.1 ± 0.1 g/cm^3, α–cellulose: 63.4%, hemicelluloses: 29.6%, lignin: 5.2%, crystallinity index: 64%, [50]) were from Azevedo Ind. Com. (São Paulo, SP, Brazil) and Pematec Triangel of Brazil Ltd. (São Paulo, SP, Brazil), respectively.

2.2. Composites Preparation

2.2.1. Internal Mixer/Thermopressing Molding

The composites were prepared following the procedures outlined in Scheme 1.

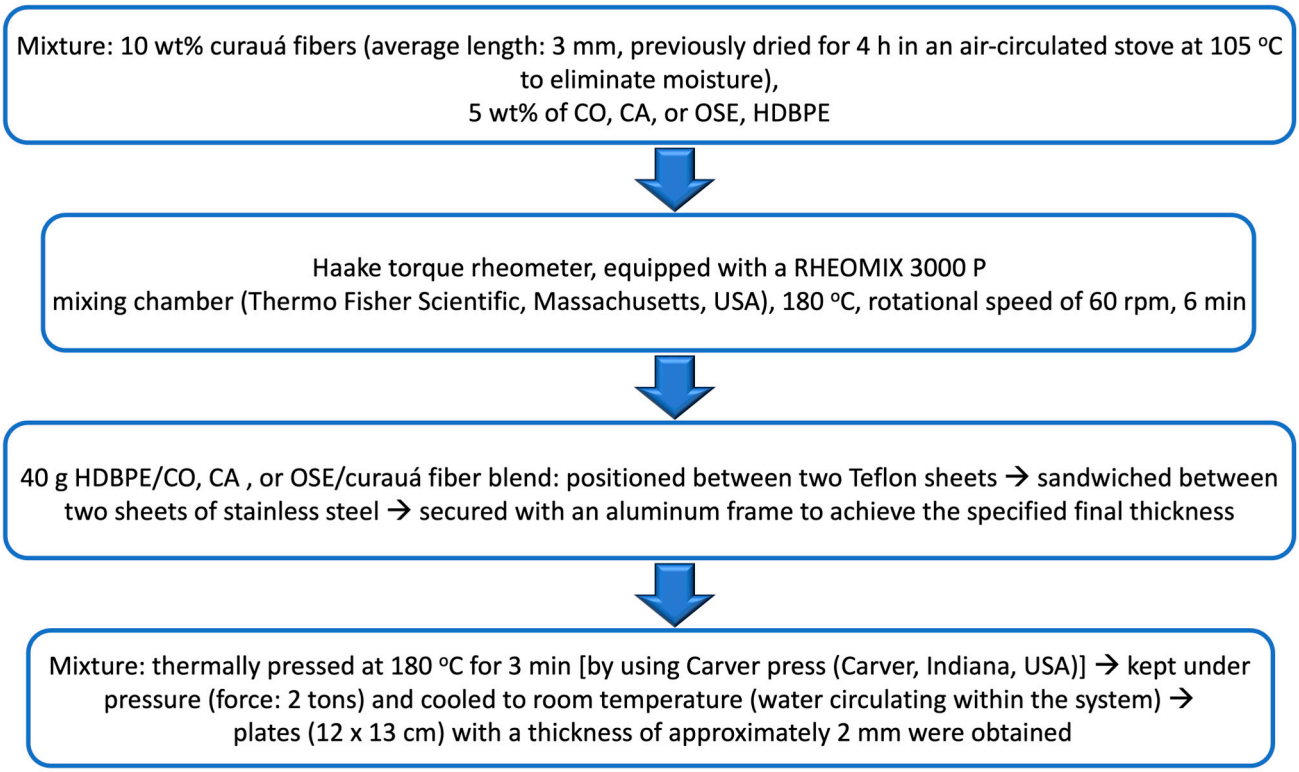

Scheme 1. Composite preparation via internal mixer/thermopressing molding.

The criteria regarding the percentages and lengths of the fibers, along with the proportion of plant-based oils, were based on the findings of a previous research study [17]. The remaining parameters demonstrated suitability throughout the investigation period.

2.2.2. Intermeshing Twin-Screw Extruder/Injection Molding

The composites were prepared per the procedures delineated in Scheme 2.

Various conditions were explored during the study's development, and those outlined in Scheme 2 were the most appropriate. The specimens underwent injection molding utilizing molds that adhere to ASTM D256 standards [51] (last updated: 1 January 2025) for impact resistance evaluation and ASTM D790-03 standards [52] (last updated: 24 July 2017) for assessing flexural properties.

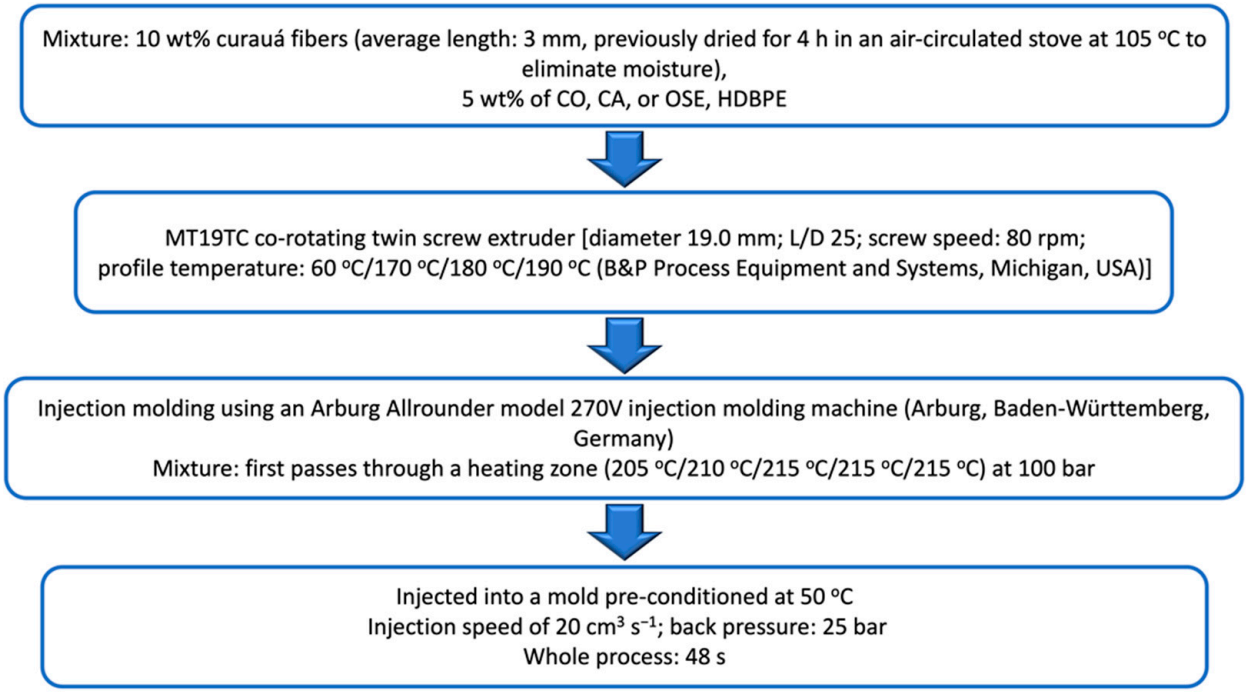

Scheme 2. Composite preparation via twin-screw extruder/injection molding.

2.3. Composites Characterization

The composites were characterized according to Scheme 3.

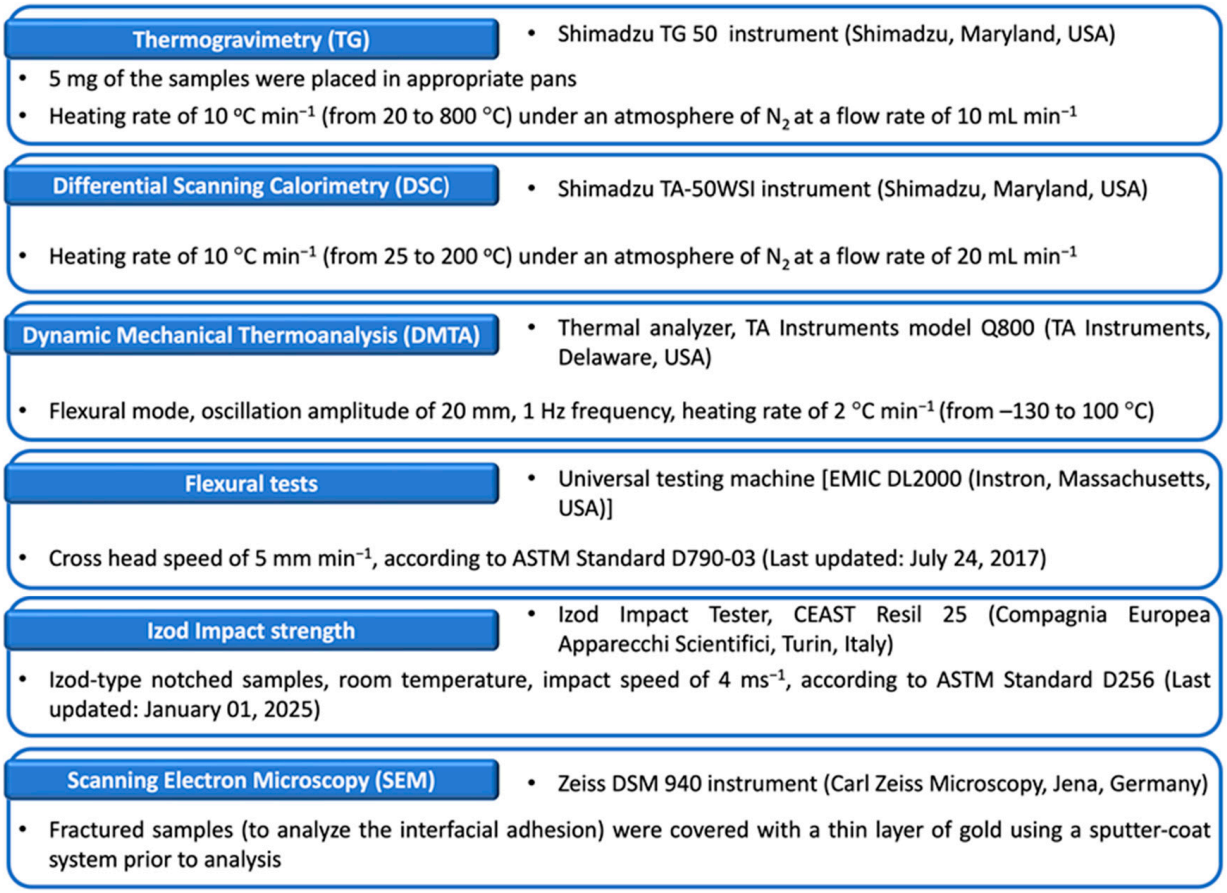

Scheme 3. Composites characterization, ASTM Standard D790-03 [52]; ASTM Standard D256 [51].

A minimum of seven specimens were utilized to assess impact and flexural strength.

3. Results and Discussion

The results reported below refer to composites obtained after mixing components using the intermeshing twin-screw extruder followed by injection molding. For comparison purposes, the results of composites obtained using the internal mixer (Haake) are shown for analyses in which the mixing methodology can impact the respective properties.

3.1. Thermal Analysis

Figure 2a displays the results of the first derivative analysis of mass loss (dTG) for the composites processed using an intermeshing twin-screw extruder, followed by injection molding. The dTG curves for HDBPE and curauá fibers are also included for comparison. The dTG curve for curauá fiber reveals a minor peak occurring below 100 °C, indicating the desorption of residual moisture. In contrast, the other materials displayed no mass loss within the temperature range of 25 °C to 100 °C, which can be attributed to the hydrophobic nature of HDBPE. A more pronounced peak at 371 °C corresponds to the thermal decomposition of cellulose, while the shoulder around 300 °C indicates the decomposition of hemicelluloses. Lignin undergoes decomposition over a broad temperature range, between 430 and 620 °C, with a peak at 526 °C [50,53,54]. In contrast, the dTG curve of HDBPE shows a peak at 493 °C. Due to the low proportion of fibers in the composites, only the mass loss associated with the most abundant component in the fibers (cellulose) is evident, peaking at 380 °C. The composites exhibit peaks at 486 °C, 489 °C, and 488 °C for the HDBPE/5%CA/10%fiber, HDBPE/5%CO/10%fiber, and HDBPE/5%OSE/10%fiber composites, respectively, indicating the thermal decomposition of HDBPE. The thermal decomposition of the vegetal-based oils was not detected in the dTG curves, attributable to their minimal proportion (5%) in the composites. The materials processed through internal mixing and thermopressing molding [17] exhibited behavior consistent with the observations detailed herein.

The endothermic peak observed at 84 °C for the curauá fibers (Figure 2b) is attributed to the volatilization of residual moisture. Peaks associated with the thermal decomposition of the fibers were not detected since the scan was terminated at 200 °C. The polymer's melting temperature in neat HDBPE and in composites comprising CO and CA was approximately 136 °C. In contrast, the composite containing OSE slightly reduced melting temperature to 131 °C. As discussed later in the analysis of the storage modulus results, it appears that OSE interacted less than CO and CA with the fibers at the fiber–matrix interface. This suggests that OSE might have engaged more with the noncrystalline regions of the polymer, particularly those adjacent to the crystalline domains; this behavior could have been preferential at elevated temperatures during scanning, facilitating greater mobility of polymer segments near the crystalline regions and potentially triggering the movement of segments within the crystalline domains. Consequently, this may have contributed to a reduction in the temperature at which melting onset occurs. The plant oil composites created through internal mixing and thermopressing exhibited melting temperatures (DSC curves not shown) comparable to pure HDBPE (Figure 2b), recorded at 136 °C (CO), 135 °C (CA), and 137 °C (OSE). In this processing method, the lower melting temperature for OSE, discernible when using the intermeshing twin-screw extruder followed by injection molding, was not observed. This may be attributed to the variations in processing temperatures and subsequent cooling inherent to each process (Schemes 1 and 2). Such differences may have influenced the crystalline domains' morphology and the compatibilizer's spatial distribution within the polymer matrix. Consequently, the compatibilizer's localization at the interfaces between the noncrystalline and crystalline phases could have varied depending

on the process used. However, the magnitude of the differences remains minor and is not expected to affect the materials' viability for future applications.

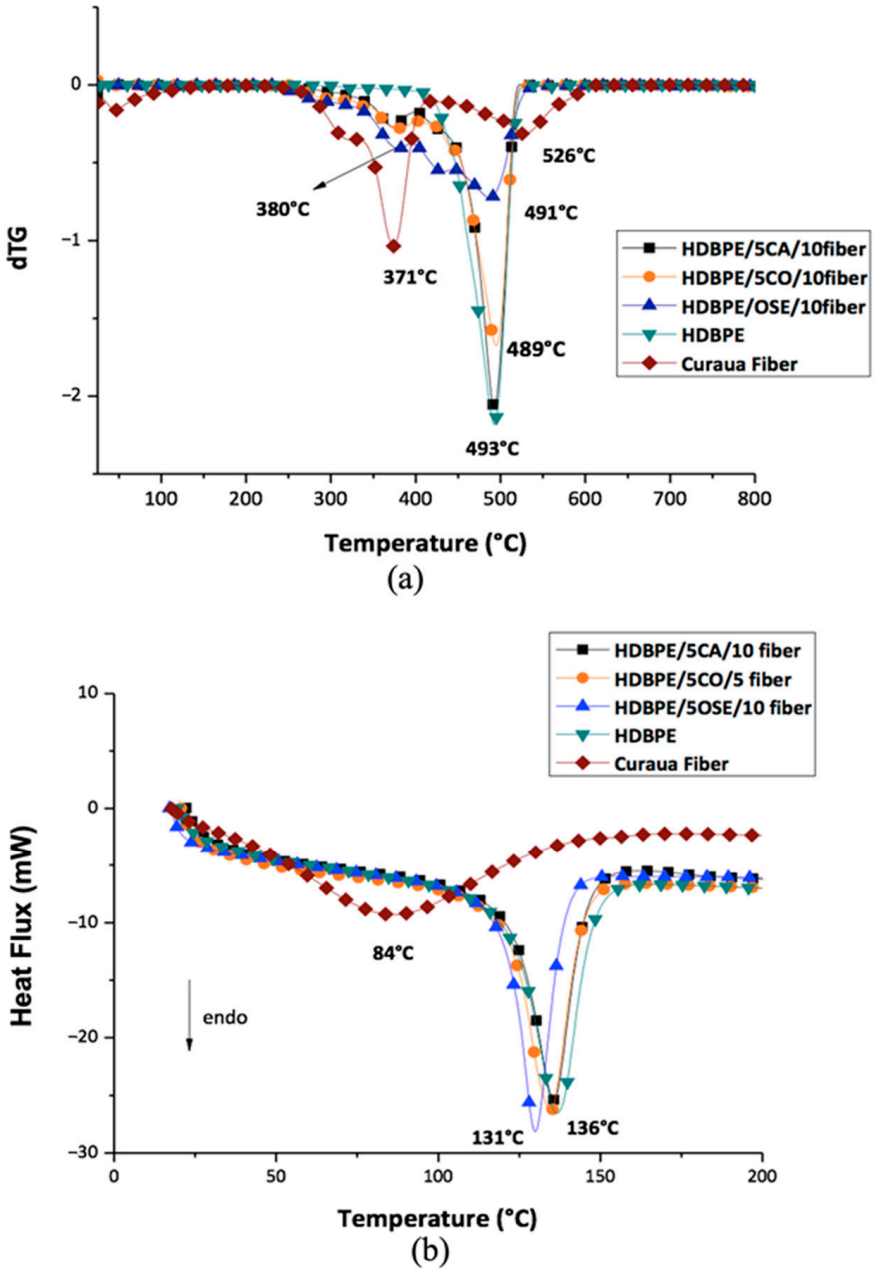

Figure 2. Curaua fiber, processed HDBPE, and curaua composites (HDBPE/5wt%CO/5wt% fiber, HDBPE/5wt%CA/10wt%fiber, HDBPE/5wt%OSE/10wt%fiber): (**a**) dTG curves, (**b**) DSC curves.

The primary objective was to assess the peak corresponding to the melting of the crystalline domains of HDBPE to calculate the crystallinity index (Xc), using $Xc = (\Delta Hm/\Delta H^{o}m\ \varphi m) \times 100$ (ΔHm: melting enthalpy of the sample, $\Delta H^{o}m$: melting enthalpy of the hypothetical 100% crystalline HDPE, 293 J/g, and φm is the mass fraction of HDBPE in the composites) [16].

Table 1 shows the calculated Xc values for the composites obtained after mixing using the extruder and the internal mixer (DSC curves not shown). The Xc value for HDBPE is also included for comparison.

Table 1. Materials crystallinity index (Xc).

Material	Xc (%)
HDBPE	67
HDBPE/5%CA/10%Fiber-extruder	84
HDBPE/5%CA/10%Fiber-internal mixer	82
HDBPE/5%CO/10%Fiber-extruder	86
HDBPE/5%CO/10%Fiber-internal mixer	85
HDBPE/5%OSE/10%Fiber-extruder	85
HDBPE/5%OSE/10%Fiber-internal mixer	84

All composites demonstrate higher degrees of crystallinity than HDBPE (Table 1), which may be attributed to the fibers acting as nucleating agents that enhance the transcrystallinity effect. This phenomenon arises from the interactions involving curauá fibers and may encompass the interactions between HDBPE and compatibilizers. As discussed later in the discussion of flexural properties, plant-based oils may also have acted as plasticizers. In this case, the mobility of the polymer chain segments is favored, which may favor ordering the segments and increase crystallinity [55].

Interestingly, there was almost no difference in the crystallinity index between the composites processed with a twin-screw extruder and those produced using an internal mixer (Table 1).

Figure 3a illustrates the impact of temperature on the storage modulus of HDBPE composites containing curauá fibers. A slight enhancement in modulus is evident in the HDBPE/5%CO/10%Fiber and HDBPE/5%CA/10%Fiber composites. This may be attributed to the increased interface stiffness resulting from stronger fiber/matrix interactions facilitated by CO and CA as compatibilizers. This fiber/matrix adhesion improvement reduces segment mobility in the interface region. In contrast, the HDBPE/5%OSE/10%Fiber composite exhibits a storage modulus curve similar to that of HDBPE alone, suggesting that the epoxy groups of OSE had minimal interaction with the polar groups of the curauá fiber components (Figure 1).

In the present study, the presence of fibers and vegetal-based oils in the composites increases the difficulty of interpreting the loss modulus curves. The peak that partially appears around –120 °C may be attributed to the movement of segments of the HDBPE chains from the noncrystalline regions, that is, the glass transition (T_g) [17]. In semicrystalline polymers, such as HDBPE, the peaks appearing at temperatures higher than T_g, involving the leathery state, correspond to segment movements between the glass and melting transition (approximately 135 °C, Figure 2) temperatures. HDBPE and its composites presented high crystallinity (Table 1), which can lead to crystalline domains with different dimensions, imposing distinct restrictions on segment movements. In this regard, peaks 2 and 3 (Table 2) are suggested to be associated with segments whose mobility is influenced by the heterogeneity and size distribution of the crystalline regions. For the composites comprising CA and CO, the interactions between the plant-derived oils and the polymer matrix may further contribute to the observed result. A more thorough analysis would require detailed DMA beyond the scope of the current study.

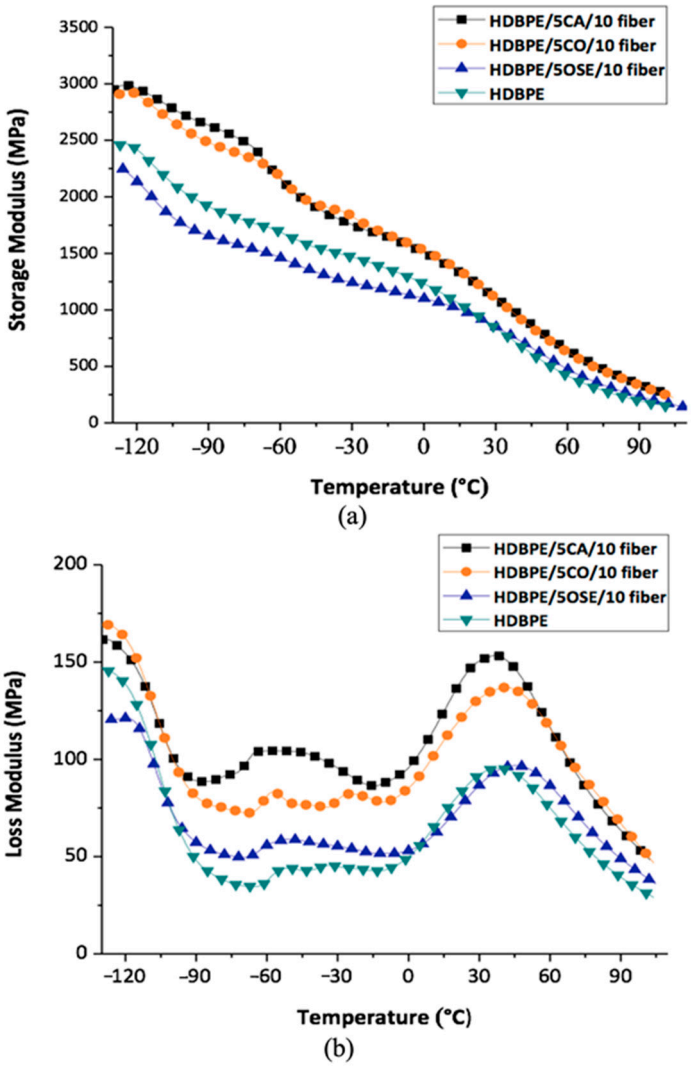

Figure 3. HDBPE and related curauá composites: (**a**) storage modulus and (**b**) loss modulus as a function of temperature.

Table 2. HDBPE and related curauá composites: DMA peaks.

	Temperature (°C)		
	Peak 1	**Peak 2**	**Peak 3**
HDBPE	−126	−50	37
HDBPE/5% CA/10% fiber	−125	−53	36
HDBPE/5% CO/10% fiber	−125	−57	40
HDBPE/5% OSE/10% fiber	−129	−51	41

3.2. Mechanical Properties and SEM Micrographs

The impact strength of the composites prepared by extrusion and injection molding was higher than that of the composite prepared by internal mixer and thermopressing (Figure 4). The conditions used during mixing in the extruder probably led to a better dispersion of the fiber and oils in the material, favoring the transfer of load from the matrix to the fiber during impact.

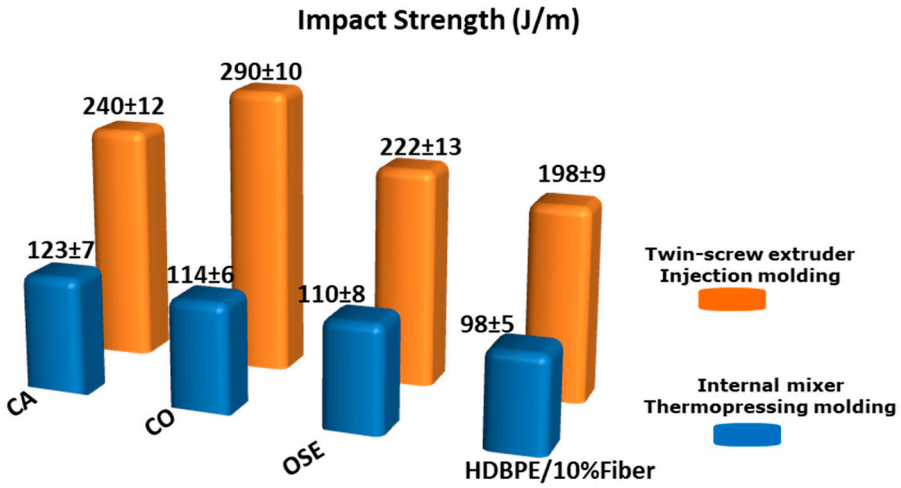

Figure 4. Izod impact strengths for HDBPE/10%Fiber, HDBPE/5%CA/10%, HDBPE/5%CO/10%, and HDBPE/5%OSE/10% curauá fiber composites (notched samples).

The compatibilizer that demonstrated the most effective performance was CO, with its composite exhibiting an impact resistance of 290 J/m (twin-screw extruder/Injection molding, Figure 4). In the absence of a compatibilizer, the material exhibited reduced impact resistance, approximately 198 J/m (HDBPE/10%Fiber, Figure 4). This diminished performance, particularly when juxtaposed with the composites containing CA and CO, is likely due to the incompatibility between the hydrophilic fibers and the hydrophobic polymer matrix. Statistically, there were no significant differences in the outcomes between the HDBPE10%Fiber and the HDBPE/5%OSE/10% formulations across both processes. CO predominantly comprises ricinoleic acid triglyceride, distinguished by its polar hydroxyl functional groups and hydrophobic domains (Figure 1). This structural characteristic fosters strong interactions with the fibers' polar constituents and the nonpolar matrix, enhancing its function as a compatibilizer. Consequently, castor oil facilitates load transfer from the matrix to the fibers, optimizing the composite's performance. It is widely recognized that the interface between the fiber and the matrix is critical in transferring load from the matrix to the fiber through, e.g., shear stress. Weak interactions at this interface can result in fiber pull-out or debonding, ultimately diminishing the composite's durability. Conversely, a robust interface can inhibit crack propagation, thereby enhancing the composite's toughness [56,57].

Figure 5 presents the micrographs of the HDBPE composites.

Micrographs a/b, d/e, and g/h illustrate the composites produced through internal mixing (Haake) followed by thermopressing. In these images, the fiber is effectively enveloped by the polymer matrix, enhancing load transfer from the matrix to the fibers, Figure 5. Conversely, micrographs c, f, and i depict composites fabricated using the twin-screw extruder and injection molding. Here, the shear forces likely led to the disaggregation of fiber bundles into smaller-diameter units, significantly increasing the surface area available for load transfer to the matrix. This morphological change is presumably the primary effect that contributed to the superior impact resistance observed in the composites processed with the twin-screw extruder and injection molding method compared to those made via internal mixing and thermopressing (Figure 4). Figure 5j,k illustrate that the absence of a compatibilizer can result in suboptimal adhesion at the fiber-matrix interface (j). This deficiency may manifest as fiber pull-out during impact (k), indicating deficiencies in interfacial interactions.

Figure 6 presents the flexural strength and modulus of the HDBPE composites. The composites did not fracture during the test and were then assessed at a strain of 5%.

Consistent with the findings from the impact strength tests, the flexural strength exhibited by the composites processed with the twin-screw extruder and subsequently molded by injection was superior compared to those produced via internal mixing and thermopressing.

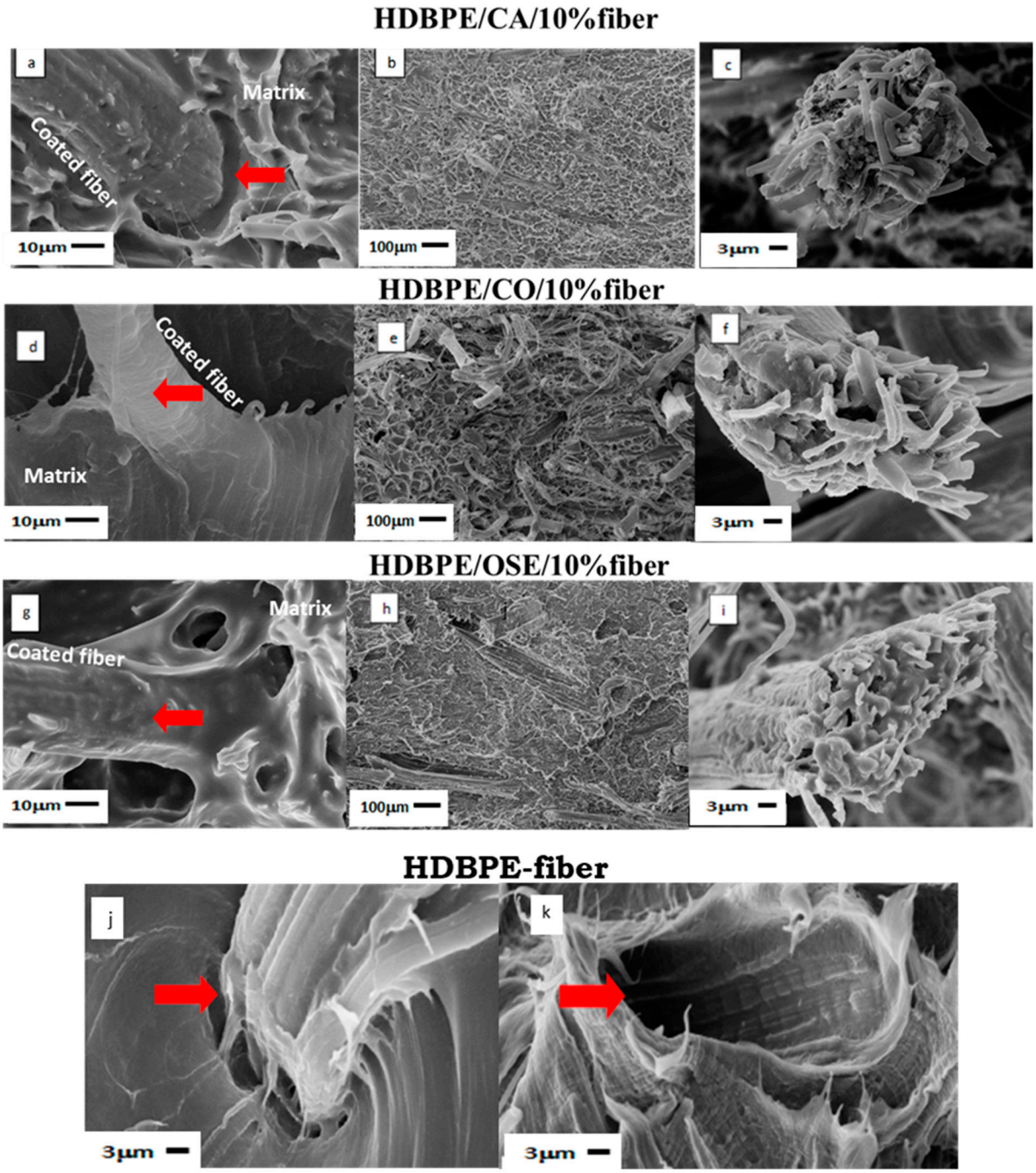

Figure 5. SEM images of fractured surfaces (after impact testing) of composites processed via internal mixer/thermopressing molding (**a**,**b**,**d**,**e**,**g**,**h**) and twin-screw extruder/injection molding (**c**,**f**,**i**). The micrographs labeled (**j**,**k**) depict the HDBPE-fiber composite.

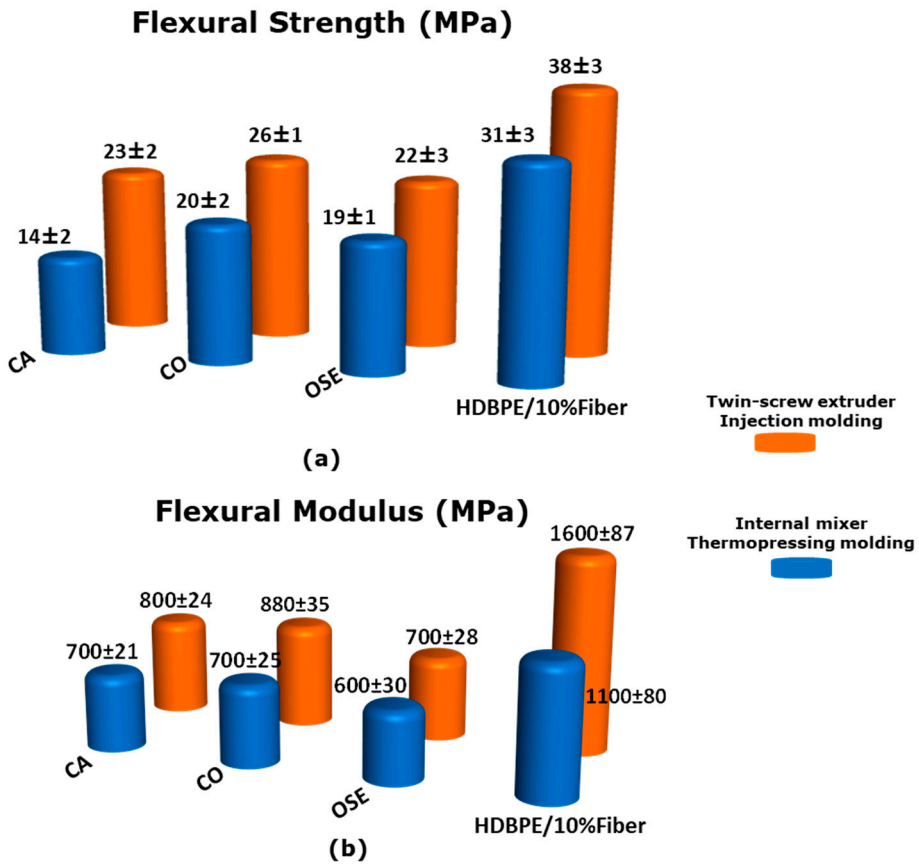

Figure 6. (**a**) Flexural strength and (**b**) flexural modulus at 5% deformation for HDBPE/10%Fiber, and HDBPE/5%CA/10%, HDBPE/5%CO/10%, HDBPE/5%OSE/10% curauá fiber composites.

The composites incorporating plant-based oils exhibited lower flexural strength and modulus at 5% deformation compared to the HDBPE/10%Fiber composite, Figure 6. In line with the International Union of Pure and Applied Chemistry (IUPAC) definition of plasticizers as substances that enhance properties like flexibility in polymers, these findings suggest that the oils functioned as plasticizers, increasing the flexibility of the materials. There is a growing trend toward utilizing plant-based oil plasticizers, which can improve composites' performance and align with sustainability in material production [29,58].

In the composites that include plant-based oils, the flexural strength at 5% strain and the modulus were higher when processed using a twin-screw extruder and injection molding instead of an internal mixer and thermopressing molding, Figure 6. For the HDBPE/10%fiber composite, this difference was mainly observed in the resistance to deformation, that is, in the modulus, Figure 6b.

Among the composites made with plant-based oils using a twin-screw extruder, the one incorporating CO exhibited slightly superior flexural strength and significantly superior modulus compared to the others (Figure 6). The analysis of the impact strength results (Figure 4) concerning the influence of CO can also be applied to interpret the flexural outcomes. The flexural modulus of the HDBPE/5%OSE/10% composite was significantly lower than the other composites. This indicates that it exhibited lower resistance to 5% deformation, suggesting that OSE primarily acted as a plasticizer rather than a compatibilizer within the composite matrix. The oxygen atoms of the epoxy rings behave only as hydrogen bond acceptors, restricting their interaction with the polar groups of the fiber components (cellulose, hemicelluloses, and lignin). Such interactions are favored for the hydroxyls present in the ricinoleic acid triglyceride (the major component of CO). This could explain the low action of OSE as a compatibilizer between HDBPE and curauá fibers.

Barbalho and co-authors [35] employed 5% curauá fibers and HDBPE grafted with 10% maleic anhydride in their study. They reported a flexural strength and flexural modulus of approximately 15 MPa and 620 MPa, respectively. Considering the results found in the present study (10% curauá fibers and 5% plant-based oil, Figure 6), it is confirmed that the use of compatibilizers from renewable sources is quite promising.

4. Conclusions

In the present study, the matrix was bio-based HDBPE, curauá reinforced the matrix, and vegetal-based oils were used as compatibilizers between fibers and the matrix. The composites were developed from raw materials characterized by a highly renewable nature, which aligns with contemporary sustainability concerns regarding the fabrication of new materials. Furthermore, substituting a portion of the polymeric components with vegetal-based fibers has the potential to lower the overall production costs of the materials.

The comparative analysis of the impact and flexural properties of HDBPE/curauá fiber/vegetal-based oil composites produced using an internal mixer followed by thermopressing *versus* those generated via a twin-screw extruder and subsequently processed through injection molding revealed that the latter methodology demonstrated significantly superior performance. The composite incorporating 5% CO exhibited the most favorable mechanical properties. The transition from an internal mixer to a twin-screw extruder increased flexural strength and modulus (at 5% of deformation) from 20 MPa and 700 MPa to 26 MPA and 880 MPa, respectively. Furthermore, the impact strength improved significantly, rising from 114 J/m to 290 J/m.

The findings of this study enabled the determination of optimal conditions for the production of composites utilizing HDBPE and curauá fibers. These established conditions may also apply to various other lignocellulosic fibers and extend to additional thermoplastic materials beyond high-density polyethylene.

In response to the growing demand for sustainability, the production of bio-based polymers is expected to increase significantly in the near future. The plant oils used in this study are readily available in many countries, and alternative oils may also be considered. Furthermore, fiber-producing plants are already cultivated widely across various regions worldwide. The methodology used for composite formation is adaptable for mass production. As a result, the strategies and findings presented in this study may act as a catalyst for the scalable production of composites derived from bio-based matrices, plant oils, and plant fibers.

Author Contributions: Conceptualization: D.O.d.C., A.C.R.-F. and E.F.; methodology: D.O.d.C., A.C.R.-F. and E.F.; software: D.O.d.C. and R.P.O.S.; validation: D.O.d.C., A.C.R.-F., R.P.O.S. and E.F.; formal analysis: D.O.d.C., A.C.R.-F., R.P.O.S. and E.F.; investigation: D.O.d.C., A.C.R.-F. and E.F.; resources: A.C.R.-F. and E.F.; data curation: D.O.d.C., A.C.R.-F., R.P.O.S. and E.F.; writing—original draft preparation: D.O.d.C., A.C.R.-F., R.P.O.S. and E.F.; writing—review and editing: D.O.d.C., A.C.R.-F., R.P.O.S. and E.F.; visualization: D.O.d.C., A.C.R.-F., R.P.O.S. and E.F.; supervision: A.C.R.-F. and E.F.; project administration: A.C.R.-F. and E.F.; funding acquisition: A.C.R.-F. and E.F. All authors have read and agreed to the published version of the manuscript.

Funding: This research was funded by the National Council for Scientific and Technological Development, Brazil (309692/2017-2 and 403494/2021-4).

Data Availability Statement: This article provides the information to understand and replicate the study's findings thoroughly.

Conflicts of Interest: Author Daniele O. de Castro was employed by the company Tetra Pak. The remaining authors declare that the research was conducted in the absence of any commercial or financial relationships that could be construed as a potential conflict of interest.

References

1. Karakaya, N.; Papila, M.; Özkoç, G. Overmolded hybrid composites of polyamide-6 on continuous carbon and glass fiber/epoxy composites: 'An assessment of the interface'. *Compos. Part A Appl. Sci. Manuf.* **2020**, *131*, 105771. [CrossRef]
2. Pan, L.; Liu, Z.; Kızıltaş, O.; Zhong, L.; Pang, X.; Wang, F.; Zhu, Y.; Ma, W.; Lv, Y. Carbon fiber/poly ether ether ketone composites modified with graphene for electro-thermal deicing applications. *Compos. Sci. Technol.* **2020**, *192*, 108117. [CrossRef]
3. Palmeri, F.; Laurenzi, S. Relaxation Modeling of Unidirectional Carbon Fiber Reinforced Polymer Composites Before and After UV-C Exposure. *Fibers* **2024**, *12*, 110. [CrossRef]
4. Szatkowski, P.; Twaróg, R. Thermal Recycling Process of Carbon Fibers from Composite Scrap—Characterization of Pyrolysis Conditions and Determination of the Quality of Recovered Fibers. *Fibers* **2024**, *12*, 68. [CrossRef]
5. Ramakrishnan, K.R.; Le Moigne, N.; De Almeida, O.; Regazzi, A.; Corn, S. Optimized manufacturing of thermoplastic biocomposites by fast induction-heated compression moulding: Influence of processing parameters on microstructure development and mechanical behaviour. *Compos. Part A Appl. Sci. Manuf.* **2019**, *124*, 105493. [CrossRef]
6. Woigk, W.; Fuentes, C.A.; Rion, J.; Hegemann, D.; Vuure, A.W.V.; Kramer, E.; Dransfeld, C.; Masania, K. Fabrication of flax fibre-reinforced cellulose propionate thermoplastic composites. *Compos. Sci. Technol.* **2019**, *183*, 107791. [CrossRef]
7. Fourati, Y.; Magnin, A.; Putaux, J.L.; Boufi, S. One-step processing of plasticized starch/cellulose nanofibrils nanocomposites via twin-screw extrusion of starch and cellulose fibers. *Carbohydr. Polym.* **2020**, *229*, 115554. [CrossRef]
8. Zamora-Mendoza, L.; Gushque, F.; Yanez, S.; Jara, N.; Álvarez-Barreto, J.F.; Zamora-Ledezma, C.; Dahoumane, S.A.; Alexis, F. Plant Fibers as Composite Reinforcements for Biomedical Applications. *Bioengineering* **2023**, *10*, 804. [CrossRef]
9. Frollini, E.; Bartolucci, N.; Sisti, L.; Celli, A. Biocomposites based on poly(butylene succinate) and curaua: Mechanical and morphological properties. *Polym. Test.* **2015**, *45*, 168–173. [CrossRef]
10. Costa, U.O.; Nascimento, L.F.C.; Garcia, J.M.; Bezerra, W.B.A.; Monteiro, S.N. Evaluation of Izod impact and bend properties of epoxy composites reinforced with mallow fibers. *J. Mater. Res. Technol.* **2019**, *9*, 373–382. [CrossRef]
11. Manimaran, P.; Saravanan, S.P.; Sanjay, M.R.; Jawaid, M.; Siengchin, S.; Fiore, V. New Lignocellulosic Aristida adscensionis Fibers as Novel Reinforcement for Composite Materials: Extraction, Characterization and Weibull Distribution Analysis. *J. Polym. Environ.* **2020**, *28*, 803–811. [CrossRef]
12. Siakeng, R.; Jawaid, M.; Asim, M. Accelerated weathering and soil burial effect on biodegradability, colour and texture of coir/pineapple leaf fibres/PLA biocomposites. *Polymers* **2020**, *12*, 458. [CrossRef] [PubMed]
13. Bessa, W.; Trache, D.; Moulai, S.-A.; Tarchoun, A.F.; Abdelaziz, A.; Hamidon, T.S.; Hussin, M.H. Polybenzoxazine/Epoxy Copolymer Reinforced with Phosphorylated Microcrystalline Cellulose: Curing Behavior, Thermal, and Flame Retardancy Properties. *Fibers* **2024**, *12*, 61. [CrossRef]
14. Da Silva, C.G.; Queiroz, B.G.; Frollini, E. Lignocellulosic biomass: Synthesis of lignophenolic thermosets with simultaneous formation of composites reinforced by sugarcane bagasse fibers. *Biomass Convers. Biorefinery* **2024**, *14*, 29503–29514. [CrossRef]
15. Mahmud, S.; Hasan, K.M.F.; Jahid, M.A.; Mohiuddin, K.; Zhang, R.; Zhu, J. Comprehensive review on plant fiber-reinforced polymeric biocomposites. *J. Mater. Sci.* **2021**, *56*, 7231–7264. [CrossRef]
16. Castro, D.O.; Marini, J.; Ruvolo-Filho, A.; Frollini, E. Preparation and Characterization of Biocomposites Based on Curaua Fibers, High-density Biopolyethylene (HDBPE) and Liquid Hydroxylated Polybutadiene (LHPB). *Polímeros* **2013**, *23*, 65–73. [CrossRef]
17. Castro, D.O.; Passador, F.; Ruvolo-Filho, A.C.; Frollini, E. Use of castor and canola oils in "biopolyethylene" curauá fiber composites. *Compos. Part A Appl. Sci. Manuf.* **2017**, *95*, 22–30. [CrossRef]
18. Da Silva, A.O.; de Castro Monsores, K.G.; de Sant' Ana, O.S.; Weber, R.P.; Monteiro, S.N.; Vital, H.C. Influence of gamma and ultraviolet radiation on the mechanical behavior of a hybrid polyester composite reinforced with curaua mat and aramid fabric. *J. Mater. Res. Technol.* **2019**, *9*, 394–403. [CrossRef]
19. Premkumar, T.; Siva, I.; Neis, P.D.; Amico, S.C.; Ferreira, F.F.; Jappes, J.T.W. Experimental design and theoretical analysis on the various tribological responses of curauá/polyester composites. *Mater. Res. Express* **2019**, *6*, 125337. [CrossRef]
20. García del Pino, G.; Kieling, A.C.; Bezazi, A.; Boumediri, H.; de Souza, J.F.R.; Díaz, F.V.; Rivera, J.L.V.; Dehaini, J.; Panzera, T.H. Hybrid Polyester Composites Reinforced with Curauá Fibres and Nanoclays. *Fibers Polym.* **2020**, *1*, 399–406. [CrossRef]
21. Zah, R.; Hischier, R.; Leão, A.L.; Braun, I. Curauá fibers in the automobile industry—A sustainability assessment. *J. Clean. Prod.* **2007**, *15*, 1032–1040. [CrossRef]
22. Araujo, J.R.; Mano, B.; Teixeira, G.M.; Spinacé, M.A.S.; De Paoli, M.-A. Biomicrofibrilar composites of high density polyethylene reinforced with curauá fibers: Mechanical, interfacial and morphological properties. *Compos. Sci. Technol.* **2010**, *70*, 1637–1644. [CrossRef]
23. Tarazona, N.A.; Machatschek, R.; Balcucho, J.; Lendlein, A.; Castro-Mayorga, J.L.; Saldarriaga, J.F. Opportunities and challenges for integrating the development of sustainable polymer materials within an international circular (bio)economy concept. *MRS Energy Sustain.* **2022**, *9*, 28–34. [CrossRef] [PubMed]

24. Quiles-Carrillo, L.; Montanes, N.; Jorda-Vilaplana, A.; Balart, R.; Torres-Giner, S. A comparative study on the effect of different reactive compatibilizers on injection-molded pieces of bio-based high-density polyethylene/polylactide blends. *J. Appl. Polym. Sci.* **2019**, *136*, 47396. [CrossRef]
25. European Environment Agency | Circularity Metrics Lab. Global Bio-Based Plastics Production Capacity. Available online: https://www.eea.europa.eu/en/circularity/sectoral-modules/plastics/global-bio-based-plastics-production-capacity (accessed on 6 February 2025).
26. Okolie, O.; Kumar, A.; Edwards, C.; Lawton, L.A.; Oke, A.; McDonald, S.; Thakur, V.K.; Njuguna, J. Bio-Based Sustainable Polymers and Materials: From Processing to Biodegradation. *J. Compos. Sci.* **2023**, *7*, 213. [CrossRef]
27. Singh, D.K.; Vaidya, A.; Thomas, V.; Theodore, M.; Kore, S.; Vaidya, U. Finite Element Modeling of the Fiber-Matrix Interface in Polymer Composites. *J. Compos. Sci.* **2020**, *4*, 58. [CrossRef]
28. Motta de Castro, E.; Tabei, A.; Cline, D.B.; Haque, E.; Chambers, L.B.; Song, K.; Perez, L.; Kalaitzidou, K.; Asadi, A. New insights in understanding the fiber-matrix interface and its reinforcement behavior using single fiber fragmentation data. *Adv. Compos. Hybrid Mater.* **2025**, *8*, 5. [CrossRef]
29. Roy, K.; Debnath, S.C.; Tzounis, L.; Pongwisuthiruchte, A.; Potiyaraj, P. Effect of Various Surface Treatments on the Performance of Jute Fibers Filled Natural Rubber (NR) Composites. *Polymers* **2020**, *12*, 369. [CrossRef]
30. Vijay, R.; Manoharan, S.; Arjun, S.; Vinod, A. Characterization of Silane-Treated and Untreated Natural Fibers from Stem of Leucas Aspera. *J. Nat. Fibers* **2020**, *18*, 1957–1973. [CrossRef]
31. Werchefani, M.; Lacoste, C.; Elloumi, A.; Belghith, H.; Gargouri, A.; Bradai, C. Enzyme-treated Tunisian Alfa fibers reinforced polylactic acid composites: An investigation in morphological, thermal, mechanical, and water resistance properties. *Polym. Compos.* **2020**, *41*, 1721–1735. [CrossRef]
32. Barbarić-Mikočević, Ž.; Bates, I.; Rudolf, M.; Plazonić, I. The Influence of Ultraviolet Radiation on the Surface Roughness of Prints Made on Papers with Natural and Bleached Hemp Fibers. *Fibers* **2024**, *12*, 112. [CrossRef]
33. Alipour, A.; Jayaraman, K. Performance of Flax/Epoxy Composites Made from Fabrics of Different Structures. *Fibers* **2024**, *12*, 34. [CrossRef]
34. Santos, R.P.O.; Ferracini, T.V.; Innocentini, M.D.M.; Frollini, E.; Savastano Junior, H. Composite electrospun membranes from cellulose nanocrystals, castor oil, and poly(ethylene terephthalate): Air permeability, thermal stability, and other relevant properties. *Int. J. Biol. Macromol.* **2025**, *287*, 138437.
35. Barbalho, G.H.A.; Nascimento, J.J.S.; da Silva, L.B.; Gomez, R.S.; de Farias, D.O.; Diniz, D.D.S.; Santos, R.S.; de Figueiredo, M.J.; de Lima, A.G.B. Bio-Polyethylene Composites Based on Sugar Cane and Curauá Fiber: An Experimental Study. *Polymers* **2023**, *15*, 1369. [CrossRef]
36. Hyvärinen, M.; Jabeen, R.; Kärki, T. The Modelling of Extrusion Processes for Polymers—A Review. *Polymers* **2020**, *12*, 1306. [CrossRef]
37. Karaki, A.; Hammoud, A.; Masad, E.; Khraisheh, M.; Abdala, A.; Ouederni, M. A review on material extrusion (MEX) of polyethylene—Challenges, opportunities, and future prospects. *Polymer* **2024**, *307*, 127333. [CrossRef]
38. Valášek, P.; Ruggiero, A.; Müller, M. Experimental description of strength and tribological characteristic of EFB oil palm fibres/epoxy composites with technologically undemanding preparation. *Compos. Part B Eng.* **2017**, *122*, 79–88. [CrossRef]
39. Hamdi, S.E.; Delisée, C.; Malvestio, J.; Beaugrand, J.; Berzin, F. Monitoring the Diameter Changes of Flax Fibre Elements during Twin Screw Extrusion Using X-Ray Computed Micro-Tomography. *J. Nat. Fibers* **2018**, *17*, 1159–1170. [CrossRef]
40. Nematollahi, M.; Karevan, M.; Fallah, M.; Farzin, M. Experimental and Numerical Study of the Critical Length of Short Kenaf Fiber Reinforced Polypropylene Composites. *Fibers Polym.* **2020**, *21*, 821–828. [CrossRef]
41. Zhao, J.; Guo, C.; Zuo, X.; Román, A.J.; Nie, Y.; Su, D.-X.; Turng, L.-S.; Osswald, T.A.; Cheng, G.; Chen, W. Effective mechanical properties of injection-molded short fiber reinforced PEEK composites using periodic homogenization. *Adv. Compos. Hybrid Mater.* **2022**, *5*, 2964–2976. [CrossRef]
42. Pheysey, J.; De Cola, F.; Martinez-Hergueta, F. Short fibre/unidirectional hybrid thermoplastic composites: Experimental characterisation and digital analysis. *Compos. Part A Appl. Sci. Manuf.* **2024**, *181*, 108121. [CrossRef]
43. Mohan, K.H.R.; Benal, M.G.M.; Pradeep, K.G.S.; Tambrallimath, V.; Geetha, H.R.; Khan, T.M.Y.; Rajhi, A.A.; Baig, M.A.A. Influence of Short Glass Fibre Reinforcement on Mechanical Properties of 3D Printed ABS-Based Polymer Composites. *Polymers* **2022**, *14*, 1182. [CrossRef] [PubMed]
44. Adapa, S.K.; Jagadish. Design and fabrication of internal mixer and filament extruder for extraction of hybrid filament composite for FDM applications. *Int. J. Interact. Des. Manuf.* **2024**, *18*, 419–432. [CrossRef]
45. Müller, D.; Bruchmüller, M.; Puch, F. Preparation of Polypropylene Composites with Pyrolyzed Carbon Fibers Using an Internal Mixer. *Recycling* **2024**, *9*, 115. [CrossRef]
46. Valente, M.; Rossitti, I.; Sambucci, M. Different Production Processes for Thermoplastic Composite Materials: Sustainability versus Mechanical Properties and Processes Parameter. *Polymers* **2023**, *15*, 242. [CrossRef]

47. Berzin, F.; David, C.; Vergnes, B. Use of Flow Modeling to Optimize the Twin-Screw Extrusion Process for the Preparation of Lignocellulosic Fiber-Based Composites. *Front. Mater.* **2020**, *7*, 218. [CrossRef]
48. Rabbi, M.S.; Islam, T.; Islam, G.M.S. Injection-molded natural fiber-reinforced polymer composites–A review. *Int. J. Mech. Mater. Eng.* **2021**, *16*, 15. [CrossRef]
49. Sriseubsai, W.; Praemettha, A. Hybrid Natural Fiber Composites of Polylactic Acid Reinforced with Sisal and Coir Fibers. *Polymers* **2025**, *17*, 64. [CrossRef]
50. Castro, D.O.; Ruvolo-Filho, A.C.; Frollini, E. Materials prepared from biopolyethylene and curaua fibers: Composites from biomass. *Polym. Test.* **2013**, *31*, 880–888. [CrossRef]
51. *ASTM D256-24*; Standard Test Methods for Determining the Izod Pendulum Impact Resistance of Plastics (Last updated: 1 January 2025). ASTM International: West Conshohocken, PA, USA, 2025. [CrossRef]
52. *ASTM D790-03*; Standard Test Methods for Flexural Properties of Unreinforced and Reinforced Plastics and Electrical Insulating Materials (Last updated: 24 July 2017). ASTM International: West Conshohocken, PA, USA, 2017. [CrossRef]
53. Hoareau, W.; Trindade, W.G.; Siegmund, B.; Castellan, A.; Frollini, E. Sugar cane bagasse and curaua lignins oxidized by chlorine dioxide and reacted with furfuryl alcohol: Characterization and stability. *Polym. Degrad. Stab.* **2004**, *86*, 567–576. [CrossRef]
54. D'Almeida, A.L.F.S.; Barreto, D.W.; Calado, V.; D'Almeida, J.R.M. Thermal analysis of less common lignocellulose fibers. *J. Therm. Anal. Calorim.* **2008**, *91*, 405–408. [CrossRef]
55. Blázquez-Blázquez, E.; Barranco-García, R.; Díez-Rodríguez, T.M.; Cerrada, M.L.; Pérez, E. Role of the plasticizers on the crystallization of PLA and its composites with mesoporous MCM-41. *J. Mater. Sci.* **2024**, *59*, 6305–6321. [CrossRef]
56. Salkind, M.J. The role of Interfaces in Fiber Composites, Chap 14. In *Surfaces and Interfaces II*; Burke, J.J., Reed, N.L., Weiss, V., Eds.; Syracuse University Press: Syracuse, NY, USA, 1968.
57. Zhou, J.; Fan, M.; Chen, L. Interface and bonding mechanisms of plant fibre composites: An overview. *Compos. B Eng.* **2016**, *101*, 31–45. [CrossRef]
58. Leite-Barbosa, O.; de Oliveira, M.F.L.; Braga, F.C.F.; Monteiro, S.N.; de Oliveira, M.G.; Veiga-Junior, V.F. Impact of Buriti Oil from *Mauritia flexuosa* Palm Tree on the Rheological, Thermal, and Mechanical Properties of Linear Low-Density Polyethylene for Improved Sustainability. *Polymers* **2024**, *16*, 3037. [CrossRef]